Access the most recent version at http://dmm.biologists.org/lookup/doi/10.1242/dmm.019844

A hypermorphic Epithelial Beta-Catenin Mutation Facilitates Intestinal Tumorigenesis in Mice in Response to Compounding WNT-Pathway Mutations

Michael Buchert[1,2,#], Franziska Rohde[3,#], Moritz Eissmann[1,2], Niall Tebbutt[2], Ben Williams[1], Chin Wee Tan[1], Alexander Owen[2], Yumiko Hirokawa[1], Alexandra Gnann[3], Gertraud Orend[4], Gayle Orner[5], Rod H. Dashwood[6], Joan K. Heath[1], and Matthias Ernst[1,2, #], Klaus-Peter Janssen[3,#]

[1] Walter and Eliza Hall Institute, Parkville, Australia, and Department of Medical Biology, University of Melbourne, Australia;

[2] Olivia Newton-John Cancer Research Institute, Heidelberg, Australia, and School of Cancer Medicine, La Trobe University, Melbourne;

[3] Department of Surgery, Klinikum rechts der Isar, Technische Universität München, Munich, Germany;

[4] Inserm U1109, MN3T team, 3 Av. Molière, 67200 Strasbourg, France; and LabEx Medalis, Université de Strasbourg, 67200 Strasbourg, France; and Fédération de Médecine Translationnelle de Strasbourg (FMTS), 67200 Strasbourg, France;

[5] University of Wisconsin, Madison, WI, United States;

[6] Texas A&M Health Science Center, Center for Epigenetics and Disease Prevention, Houston, TX, United States.

# equal contributions by these authors

Correspondence:

Michael Buchert, PhD
Olivia Newton-John Cancer Research Institute
145 Studley Road
Heidelberg, VIC 3084, Australia
tel: +61-3-9496-5878
E-mail: michael.buchert@onjcri.org.au

Klaus-Peter Janssen, PhD
Dept. of Surgery / MRI
Ismaninger Str. 22
81675 Munich, Germany
tel: +49-89-4140-2066
E-mail: klaus-peter.janssen@lrz.tum.de

Keywords: colorectal cancer, mouse models, gpA33, inflammation

ABSTRACT

Activation of the Wnt/β-catenin pathway occurs in a vast majority of colorectal cancers. However, the outcome of the disease strongly varies from patient to patient, even within the same tumor stage. This heterogeneity is governed in large parts by the genetic makeup of individual tumors and the combination of oncogenic mutations.

To express throughout the intestinal epithelium a degradation resistant β-catenin (*Ctnnb1*) which lacks the first 131 amino acids, we inserted an epitope-tagged ΔN(1-131)-β-catenin encoding cDNA as a knockin transgene into the endogenous *gpA33* gene locus in mice. The resulting *gpA33*$^{\Delta N\text{-}Bcat}$ mice show increased constitutive Wnt/β-catenin pathway activation that shifts the cell fate towards the Paneth cell lineage in pre-malignant intestinal epithelium. Furthermore, 19% of all heterozygous and 37% of all homozygous *gpA33*$^{\Delta N\text{-}Bcat}$ mice spontaneously develop aberrant crypt foci and adenomatous polyps, at frequencies and latencies akin to that observed in sporadic colon cancer in humans. Consistent with this, the Wnt target genes, MMP7 and Tenascin-C, which are expressed highest in benign human adenomas and early tumor stages, were up-regulated in pre-malignant tissue of *gpA33*$^{\Delta N\text{-}Bcat}$ mice, but not those Wnt target genes associated with excessive proliferation (i.e Cdnn1, c-myc). We also detected diminished expression of membrane-associated α-catenin and increased intestinal permeability in *gpA33*$^{\Delta N\text{-}Bcat}$ mice under challenged conditions, providing a potential explanation for the observed mild chronic intestinal inflammation and increased susceptibility to azoxymethane and mutant *Apc*-dependent tumorigenesis. Collectively, our data indicate that epithelial expression of $\Delta N_{(1\text{-}131)}$-β-catenin in the intestine creates an inflammatory microenvironment and cooperates with other mutations in the Wnt/β-catenin pathway to facilitate and promote tumorigenesis.

INTRODUCTION

Colorectal tumorigenesis is promoted by chronic inflammation of the intestine, and patients suffering from Crohn's disease or ulcerative colitis have an increased risk of developing colorectal cancer. The canonical Wnt/β-catenin signaling pathway is aberrantly activated in the majority of colorectal cancers. Mutations of the *APC* (*adenomatous polyposis coli*) gene are the most common form of genetic alteration in CRC and represent the earliest detectable genetic change in tumorigenesis (Jen et al., 1994; Powell et al., 1992; Smith et al., 1994). Most of the tumor suppressing functions of *APC* are attributed to its capacity to negatively regulate β-catenin, a central component of the canonical Wnt/β-catenin signaling pathway (Polakis, 1997; Polakis, 2000). Accordingly, *APC* impairment mutations, epigenetic silencing (Dimberg et al., 2013; Gay et al., 2012; Qiu et al., 2014) or amino terminal mutations in *CTNNB1* mutations that result in excessive stabilization and nuclear accumulation of β-catenin result in excessive TCF/LEF-dependent transcription and associated neoplastic transformation and intestinal adenoma formation. Besides their role in the canonical Wnt/β-catenin pathway, APC also regulates cell migration, adhesion, chromosome segregation, spindle assembly and apoptosis (Dikovskaya et al., 2007; Hanson and Miller, 2005). Meanwhile, a pool of β-CATENIN localises at the cell membrane to maintain integrity of cell-cell adherens junctions by linking E-CADHERIN to α-CATENIN and the actin cytoskeleton (Lilien and Balsamo, 2005).

The various APC truncation mutations identified suggest molecular complexity of the mechanism(s) by which deregulated Wnt/β-catenin signaling drives intestinal tumor formation. For instance, Apc^{1638N} mice express undetectable levels of C-terminal truncated Apc protein and carry 5-6 tumors by 10 months of age, whereas Apc^{Min} mice develop more tumors with a shorter latency period, which is preceded by the obligatory loss of Apc heterozygosity (Fodde et al., 1994; Luongo et al., 1994). Similarly, enforced expression of an

amino-terminally truncated β-catenin that lacks the 76 amino acids encoded by exon 3 leads to the formation of numerous adenomatous polyps in the small intestine and some microadenomas in the colon (Harada et al., 1999, Leedham et al., 2013). However, calbindin promoter-dependent overexpression of the more severe ΔN131β-catenin truncation mutant results in multifocal dysplastic lesions in the small intestine after 3-4 weeks, with mice succumbing prematurely to polycystic kidney disease (Romagnolo et al., 1999). A shared feature of the above models is there propensity to develop the majority of large number of tumors in the small intestine, rather than the few early tumors in the colon of the majority of humans of age 50+ that bear the risk to ultimately develop into sporadic metatstatic CRC. IN an effort to address these shortcomings, we developed a novel knockin mouse model that exploits the intestine-specific *gpA33* gene locus to enforce expression of a ΔN131β-catenin encoding transgene throughout the epithelial mucosa. Surprisingly, the corresponding *gpA33*$^{\Delta N\text{-}Bcat}$ mice show a mild decrease in epithelial barrier function associated with elevated expression of inflammatory cytokines prior to the spontaneous development of a small number of, primarily colonic, tumors developing in aging mice. We therefore propose that *gpA33*$^{\Delta N\text{-}Bcat}$ mice can serve to investigate the compounding pathophysiological consequences of reduced barrier function, ensuing inflammation and oncogenic driver mutations in the colon, as well as serving as a model for the development of novel chemopreventive and/or therapeutic strategies (Orner et al., 2002).

RESULTS

ΔN-Bcat is expressed in intestinal epithelial cells of gpA33$^{\Delta N\text{-}Bcat}$ mice

The gpA33 antigen is a glycosylated transmembrane protein that is expressed specifically in the intestinal epithelium (Catimel et al., 1996; Heath et al., 1997; Johnstone et al., 2000). We exploited the endogenous *gpA33* gene locus to drive intestinal-specific expression of an N-terminal deletion mutant of β-catenin (ΔN-Bcat) encoded by a bicistronic gpA33-IRES-ΔN-βcatenin RNA (Supplementary material Fig. S1A,E). For this, a cDNA encoding ΔN(1-131)β-catenin, in which a FLAG epitope replaced the first 131 amino terminal amino acids, was inserted in the 3' UTR of the *gpA33* antigen gene locus (Orner et al., 2002). As *gpA33* is also transcribed in embryonic stem cells, we blocked the transcription of ΔN-Bcat by a lox(P)-flanked neo cassette in the corresponding *gpA33*^{Neo} (henceforth referred to as A33Neo) mouse strain. Transcriptional activation of the silent ΔN-Bcat transgene was achieved by excising the lox(P)-flanked neo cassette in the germline to yield the *gpA33*$^{\Delta N\text{-}Bcat}$ (henceforth referred to as Bcat) strain (Supplementary material Fig. S1A).

To verify tissue-specific expression of ΔN-Bcat, we performed qRT-PCR analysis on different tissues in A33Neo and Bcat mice. We detected ΔN-βcatenin mRNA in the small and large intestines of Bcat mice but not in liver or in intestines of A33Neo mice (Supplementary material Fig. S1C). Transcript levels of the truncated β-catenin were higher in the large intestine as predicted from the rostro-caudal expression gradient of endogenous gpA33 (supplementary material Fig. S1D). We confirmed by Northern blot and anti-FLAG immunoprecipitation analysis that Bcat transgene expression occurred in a gene dose-dependent manner (Supplementary material Fig. S1E,K) and that it did not affect expression of endogenous β-catenin in Bcat mice (Supplementary material Fig. S1B). We also ascertained nuclear accumulation of ΔN-βcatenin by subcellular fractionation of intestinal

lysates from Bcat mice (Supplementary material Fig. S1H). As predicted from the introduced truncation mutations, immunoprecipitation with an anti-E-cadherin antibody furthermore confirmed that ΔN-βcatenin retained the capacity to bind to E-cadherin at the membrane (Supplementary material Fig. S1I). The expression level of the mutant ΔN-βcatenin was approximately 50% compared to endogenous β-catenin in total lysate and further reduced to about 30% in the nuclear compartment (Supplementary material Fig. S1F-H).

Increased number of Paneth cells in Bcat mice

To evaluate the capacity of ΔN-βcatenin to regulate Wnt target genes, we performed qRT-PCR analysis on small and large intestinal tissue of wild type (Wt) and Bcat mice. Although expression of the constitutive active delta-exon 3 β-catenin mutant results in elevated expression of the prototypical Wnt target genes c-myc, cyclinD1 and CD44, expression of these genes remained unaffected in Bcat mice (Fig. 1A-C). In agreement with this, we found similar staining patterns for the proliferation marker Ki67 in the crypts of Lieberkühn in Bcat and Wt mice (Fig. 1D,E). However, in the small intestine of Bcat mice we detected a significant increase of the Paneth-cell specific transcripts encoding matrix metalloproteinase 7 (MMP7) and cryptidin 1 and this coincided with a significant expansion in the staining zone of Ulex Europaeus Agglutinin lectin (UEA) and lysozyme positive cells (Fig. 1F-I). Collectively, these observations indicate a gradient whereby limited overexpression of a stabilized ΔN-βcatenin can selectively shift the cell fate towards the Paneth cell lineage as described (Andreu et al., 2008; van Es et al., 2005), but without increasing the rate of mucosal renewal associated with excessive activation of the Wnt target genes c-myc and cyclinD1.

Inflammatory cytokines in Bcat mice

Expression of (ΔN28-134)β-catenin results in loss of intercellular adhesiveness (Oyama et al., 1994) in the human gastric signet ring cell carcinoma cell line HSC-39 through impaired interaction between mutant β-catenin, α-catenin and E-cadherin. However we found no overt mislocalization of membrane bound E-cadherin in cultures of intact colonic crypts isolated from Bcat mice, consistent with our biochemical analysis and the prediction that ΔN-Bcat protein retains its E-cadherin interaction domain (Fig. 2A,B, Supplementary material Fig. S1I). Since we detected increased β-catenin expression in the nucleus, cytosol and membrane fraction of isolated intestinal epithelium (Fig. 2B) that was associated with the expected reduction of α-catenin levels, as determined by WB and IF staining in the colon of Bcat mice (Fig. 2C-E), suggesting that ΔN-Bcat interfered with the formation of a functional α-catenin/β-catenin/E-cadherin complex at the membrane. To investigate likely physiological consequences of aberrant formation of such membrane complexes, we measured intestinal permeability in ΔN-Bcat mice using TRITC-labelled dextran (TD) gavage and observed leakage from the intestinal lumen into the circulation through serum TD quantitation 4 hours later. While the permeability to 4kDa TD remained comparable between unchallenged Wt and Bcat mice, we noted increased leakiness of the intestinal mucosa of Bcat mice when challenged by limited exposure to the luminal irritant Dextran Sulfate Sodium (DSS) for 16 hours (Fig. 2F). Following administration of 2% DSS in drinking water, Bcat mice demonstrated a significant increase in serum TD suggesting their intestinal mucosa's underlying sensitivity to reduced barrier function. However, the increase in the inflammatory cytokines IL-17 and IL-23 (Fig. 2G) alongside the reduced expression of α-catenin (Fig. 2C-E) present already in the unchallenged colons of Bcat mice implies influx of innate immune cells (Grivennikov et al., 2012) possibly due to increased permeability to molecules smaller than TD.

Spontaneous, sporadic colonic tumor formation in Bcat mice

Although stronger alleles of mutant β-catenin rapidly induce extensive epithelial hyperproliferation and formation of up to several hundreds adenomas primarily in the small intestine of mice (Harada et al., 1999; Leedham et al., 2013), tumor formation in these mice neither reflects tumor latency, multiplicity nor site where the majority of adenomas arise in humans from which CRC ultimately develops. We therefore determined spontaneous tumor occurrence in old (8-24 month) Bcat mice and found that 22 of 54 (37%) homozygous mice carried macroscopically visible colonic tumors at an average rate of 1.7 tumors per mouse. Predictably, spontaneous tumor formation was smaller in heterozygous mice where only 6 of 31 (19%) mice showed macroscopically visible adenomas (1.5 tumors per mouse) (Supplementary material Table S1). Meanwhile, none of the age-matched wild type littermate mice (n=18) showed any sign of intestinal lesions. Most of the detected lesions in homozygous Bcat mice comprised relative small colonic adenomas (<1.0mm), however, we also occasionally detected in old mice (>22 months) larger adenoma (1.9-2.7 mm diameter). Histopathological analysis revealed that all tumors in Bcat mice corresponded to hyper-proliferative tubular adenoma with equally sized cell nuclei and a prominent desmoplastic reaction (Fig. 3A). Furthermore, β-catenin was diffusely localized throughout the cytosol and nuclei of tumor cells, but clearly remained associated with the plasma membrane in adjacent normal epithelium. Meanwhile, non-uniform organization of F-actin was observed throughout tumors, and these lesions also stained strongly for UEA and lysozyme, and prominently for Ki67 (Fig. 3A). Consistent with this, the Paneth cell marker MMP7, which was among the few Wnt-target genes deregulated in the normal epithelium of Bcat mice (Fig. 1G), was already significantly up-regulated in benign human colonic adenoma (Fig. 3B). Like MMP7, Tenascin-C, another Wnt target gene, is also upregulated in the normal mucosa of Bcat mice (Fig. 3C-E), and this persists in the tumor of these mice and in human human colorectal cancer samples (n=31) (Supplementary material Fig. S2A,B). Consistent with the expression

of MMP7 and Tenascin-C being highly sensitive to Wnt pathway activation, we also detected up-regulation of these genes within the tumors of Apc mutant mice. (Fig. 3C,G).

Bcat mice are sensitized to AOM-induced tumorigenesis

To establish whether expression of the ΔN-Bcat transgene sensitized mice to chemical tumorigenesis, we challenged Bcat mice with the organotropic carcinogen azoxymethane (AOM). Mice were then analysed 5 and 12 weeks after the last of 6 consecutive AOM injections and colons were stained in methylene blue to identify ACFs (McLellan and Bird, 1988). Compared to Wt mice, Bcat mice harboured more ACFs and more adenomatous polyps (Fig. 4A-C,E), which however consistently remained well differentiated (Fig. 4D).

In order to gain insights into the molecular events underpinning the cooperation between the *ΔN-βcatenin* allele and AOM, we determined the nucleotide sequences of the mutagen hotspots in the endogenous *Kras* and *ctnnb1* genes. We found similar frequencies of activating missense mutations affecting codons 12, 13 and 61 of the *Kras* gene in tumors of Wt and Bcat mice. However, only tumors of Bcat mice (4 of 24) carried missense mutations in the *ctnnb1* codons that substituted the regulatory serine residues at positions 37 and 38 (Supplementary material Table S2) to result in stabilized more active form of βcatenin. In order to determine whether AOM also introduced functionally equivalent nonsense mutations in the *Apc* gene that result in a truncated, less stable or non-functional Apc protein, we stained tumor sections with an antibody that specifically recognizes a C-terminal epitope of the Apc protein. We observed weaker Apc staining in a much larger proportion of adenomas from Bcat than from Wt mice (Supplementary material Table S2 and data not shown). Collectively, these results suggested that AOM-induced somatic mutations that further activate the Wnt/β-catenin pathway (i.e. gain-of-function mutations in *ctnnb1*; loss of function mutations in *Apc*),

rather than mutations in the Ras-Erk signalling cascade, co-operate with ΔN-Bcat to trigger intestinal tumorigenesis.

Level of tumorigenesis differs in mouse models for colorectal cancer

We previously showed that concomitant mutations in *Apc* and *Kras* increased intestinal tumorigenesis and mortality of compound pVillin-*Kras*^{V12G};*Apc*^{1638N} mice, where the *Apc*^{1638N} allele alone, upon loss of heterozygosity of the remaining wild type *Apc* allele, confers development of 3-4 tumors per mouse (Janssen et al., 2006). Similar observations have also been reported in *Kras*^{V12G} compound mutant mice based on the stronger *Apc*^{Min} allele (Luo et al., 2009). We reconciled these observations, at least in part, by the ability of oncogenic *Kras*^{V12G} to enhance accumulation of nuclear β-catenin and hence to further activate canonical Wnt/β-catenin signaling. To better understand the molecular mechanisms underlying the functional discrepancy between co-operations of ΔN-Bcat with the AOM-induced Apc and Kras mutations, respectively, we generated compound mutant pVillin-*Kras*^{V12G};*gpA33*$^{\Delta N\text{-}Bcat}$ mice (referred to as Ras/Bcat), *Apc*^{1638N};*gpA33*$^{\Delta N\text{-}Bcat}$ mice (referred to as 1638N/Bcat) and *Apc*^{Min};*gpA33*$^{\Delta N\text{-}Bcat}$ mice (referred to as Min/Bcat). Consistent with our results from the AOM challenge, we observed that the homozygous *ΔN-Bcat* allele conferred a small additive effect in the compound Ras/Bcat mice yielding an average of 4 tumors per mouse compared to 1.7 and 2.3 tumors observed in the corresponding single mutants (Table 1). By contrast, ΔN-Bcat conferred synergistic effects on both *Apc* mutant alleles, averaging 7.8 tumors per 1638N/Bcat mouse and 62.5 tumors per Min/Bcat mouse compared to 3.9 tumors per Apc^{1638N} and 22.3 tumors per Apc^{Min} mouse. There were no gross morphological and histological differences between the lesions of the compound mutant mice, which comprised mainly well-differentiated adenomas (Supplementary material Fig. S3). Likewise, overall tumor incidence remained independent of the presence of the *ΔN-Bcat* allele (Table 1). Thus,

ΔN-Bcat promotes intestinal polyposis in Apc mutant backgrounds in a synergistic manner whereas it merely shows additive effects in mutant Kras animals.

Establishment of a pro-angiogenic environment in the intestines of Bcat mice

To better understand the molecular mechanisms that are likely to underpin the effects of the ΔN-Bcat mutation on intestinal tumor multiplicity, we monitored expression of the Wnt/β-catenin target gene *c-myc* and *Ccnd1*, which serve as a gate-keeper in Apc-dependent tumor formation (Sansom et al., 2007) and promote cell cycle progression, respectively. Surprisingly, expression of c-myc and cyclinD1 in tumors remained unaffected irrespective of whether they also harbored the ΔN-Bcat mutation, and irrespective of whether they were associated with the mutations in *Kras* or *Apc* (Fig. 5 A,B). Consistent with this, the average tumor size remained similar upon addition of the ΔN-Bcat mutation (Table 1). However in the lesions of Min/Bcat compared to the other mouse models, the ΔN-Bcat allele conferred a strikingly increased expression of osteopontin (OPN) and Cox2 (Fig. 5 C,D), which can be considered as surrogate markers for activation of the Wnt/β-catenin pathway and inflammation (Araki et al., 2003; Mitra et al., 2012). We confirmed these findings by immunofluorescence staining of Cox2, which revealed significantly more Cox2 positive cells in tumors of Ras/Bcat and 1638N/Bcat mice than in tumors of their single *Apc* and Ras mutant counterparts (Fig. 6A,B). Strikingly, the Cox2 staining was more prominent in the tumor stroma than the epithelial tumor compartment. Since Cox2 activity has been linked to increased tumor angiogenesis, we also stained tumor sections with the endothelial cell marker CD31 and observed a significant increase in CD31 positive blood vessels in tumors of 1638N/Bcat and Min/Bcat mice, but not in tumors of Ras/Bcat mice (Fig. 6C-F). Collectively these observations suggest that the ΔN-Bcat mutation co-operates with Apc mutations, which further activate the Wnt/β-catenin pathway to help establishing a pro-angiogenic environment conducive to promote intestinal tumorigenesis.

DISCUSSION

We have generated a new *gpA33*$^{\Delta N\text{-}Bcat}$ knockin mouse model to study intestinal tumor susceptibility by inserting the 1-131 amino-terminally truncation mutant of β-catenin into the 3'UTR of the endogenous *gpA33* antigen locus. Expression of this ΔN-Bcat transgene *per se* resulted in the formation of primarily colonic tumors in 37% of all Bcat mice of at least 8 months of age, akin to the long latency and low penetrance observed in human sporadic CRC. Our observations that ΔN-Bcat expression functionally co-operates with loss-of-function mutations in *Apc* rather than gain-of-function Kras mutations, implies the existence of a minimal threshold level for canonical Wnt/β-catenin signaling to trigger tumor formation (Albuquerque et al., 2010; Buchert et al., 2010; Leedham et al., 2013; Roose et al., 1999; Samuel et al., 2009). Indeed, in Bcat mice we detected transcriptional activation of only a subset of Wnt/β-catenin target genes, including some specific for Paneth cells. This is consistent with models suggesting that different gene promoters require different levels of Wnt/β-catenin pathway activation for efficient transcription (Albuquerque et al., 2010; Darken and Wilson, 2001), and mathematical calculations that the combination of gene specific regulatory mechanisms with gradients of β-catenin and Apc functions are sufficient to confer distinct target gene expression patterns (Benary et al., 2013).

Functionally, Paneth cells contribute to intestinal homeostasis by providing niche factors to retain the stemness of Lgr5 positive intestinal cells. While the latter population also contributes the cells of origin for intestinal tumors (Barker et al., 2009), human colonic neoplasms are frequently characterized by excessive abundance of Paneth(-like) cells (Joo et al., 2009). Likewise**,** the serum levels of Tenascin-C and MMP7 are increased in patients with CRC and have been proposed as biomarkers for primary and metastatic CRC, respectively (Pryczynicz et al., 2013; Takeda et al., 2007). Moreover, Tenascin-C is increasingly

recognised to play an important role in shaping the tumor microenvironment (Spenle C, Cell Adh Migr 2015 Jan 22:0). However, we noted that the increase in Paneth cells in Bcat mice was not accompanied by an increase in stem cells markers Lgr5, Sox9 or Ascl2 in the normal intestine, nor activation of the Notch pathway (Supplementary material Fig. S4 A-C, and data not shown), which also regulate cell fate decisions in the intestine. Likewise, in Bcat mice we did not observe the increase in progenitor cell proliferation characteristically observed when the Wnt/β-catenin pathway is maximally stimulated following biallelic *Apc* inactivation (Sansom et al., 2006).

Several studies have reported the effects of intestinal expression of N-terminal mutants of β-catenin *in vivo*. The most extensive intestinal hyperproliferation and adenoma formation resulted from Cre-mediated excision exon 3 (encoding amino acids 5-80) of the endogenous *ctnnb1* gene throughout the intestinal mucosa, thereby deleting all the regulatory serine and threonine residues that control the turnover of the β-catenin protein (Harada et al., 1999; Leedham et al., 2013). By contrast, mice that transgenically expressed β-catenin lacking amino acids 1-89 (Wong et al., 1998) remained tumor-free at 10 month of age, but developed abnormal villus branching in the small intestine consistent with the rostro-caudal gradient of *Fabpl* gene promoter used to drive the transgene. Meanwhile, ubiquitous expression of a doxycycline-inducible version of the same β-catenin transgene resulted in rapid expansion of the intestinal crypt compartment, mislocalization of Paneth cells and upregulation of many Wnt target genes (Jarde et al., 2013). Transgenic expression of ΔN131β-catenin under the control of the calbindin promoter resulted in intestinal tumors strictly confined to the small intestine, and premature death associated with transgene-induced polycystic kidney disease (Romagnolo et al., 1999). Here we show that expression of the same version of □-catenin, albeit as a homozygous knockin transgene and under the control of the *gpA33* locus, results primarily in colonic tumors without detrimental effects in other organs. Notwithstanding the

different nature of the various β-catenin truncation mutations in the above models, we interpret the different biological outcomes primarily as a consequence of the different spatial expression patterns, conferred to by the various gene promoters, and "signaling strength" as a function of the gene promoter and the nature of the β-catenin mutation. For instance, in their doxycycline-inducible model Jarde *et al* noted that transgene expression exceeded that of the endogenous *ctnnb1* gene by up to 11,000 fold (Jarde et al., 2013), while in our Bcat mice the level of ΔN-Bcat expression remains more comparable to that of the simultaneously expressed endogenous wild type protein. It remains to be determined whether the presence of the amino-terminal FLAG-tag and the associated introduction of bulky amino acids immediately following the 3'-end of the IRES account for moderate expression from the second cistron of the gpA33-IRES-ΔN-Bcat RNA (Bochkov and Palmenberg, 2006). Thus in general, activation of Wnt/β-catenin pathway in Bcat mice falls short of reaching the threshold required to induce adenoma formation in the colon, but predisposes these mice to tumorigenesis upon exposure to mutant *Apc* alleles or AOM-induced mutations in components of the Wnt signaling pathway. Bcat mice are therefore likely to provide a background that is genetically sensitized for the functional detection and confirmation of mutation variants in components of the canonical Wnt/β-catenin pathway.

Changes to intestinal permeability have recently been recognized as a contributing factor to intestinal mutagenesis. Here we show that relative modest activation of the Wnt/β-catenin pathway increased intestinal permeability prior to formation of adenomas, and the former is likely to account for the increased expression of the pro-inflammatory proteins Cox2, osteopontin, IL-17 and IL-23.

We speculate that this may result from the impaired interaction of ΔN-Bcat with α-catenin, which is likely to weaken the interaction of the actin cytoskeleton with the plasma membrane

in intestinal epithelial cells. Our observations suggest that oncogenic activation of the canonical Wnt/β-catenin pathway may help to set up a pro-tumorigenic microenvironment that precedes subsequent neoplastic transformation of the epithelium. This may be further exaggerated once tumors are established, since the leakiness in *Apc* mutant colonic adenomas in mice triggered further accumulation of IL-17 and IL-23 in the tumor stroma (Grivennikov et al., 2012). Interestingly, cytoplasmic and nuclear β-catenin accumulation is detected in the majority of pre-neoplastic intestinal epithelium of IBD patients (Claessen et al., 2010; van Dekken et al., 2007). Meanwhile, the importance of the IL-17/IL-23 axis is well documented for the pathogenesis of Crohn's disease and ulcerative colitis in humans (Clevers, 2006), and Cox2-derived lipids, including prostaglandin E2, are potent inflammatory mediators that promote tumor growth and metastasis (Wang et al., 2005; Xia et al., 2012). Conversely, for the non-transformed epithelium it is intriguing to speculate that the Wnt-signaling-dependent increase in Paneth cells and their transcripts is part of the epithelium's response to increased bacterial antigen exposure. Upregulation of cryptidin 1 in the intestine of Bcat mice, for instance, is consistent with the upregulation of α-DEFENSIN 5 and 6 in the leaky and inflamed colons of patients with ulcerative colitis (Supplementary material Fig. S5).

In conclusion, the Bcat mice provide a model, to mimics some of the critical aspects of sporadic CRC induction in humans in terms of tumor multiplicity, tumor latency, tumor site specificity, and coincides with upregulation of the earliest markers for human emerging CRC in humans, including Tenascin-C, MMP-7, OPN and COX2.

MATERIALS AND METHODS

Animal Models

All experiments on mice were performed in accordance with institutional and national guidelines and regulations. Mice were maintained by crossing to C57Bl/6J animals. To control for genetic background effects, littermates were always used as controls. Mice were maintained under a 12-hour light-dark cycle and fed with standard diet and water ad lib. The *Apc*^{Min}, *Apc*^{1638N} and the pVillin-*Kras*^{G12V} models have been published previously (Janssen et al., 2006; Smits et al., 1998; Su et al., 1992).

Generation of the *gpA33*$^{\Delta N\text{-}Bcat}$ mouse

The *gpA33*$^{\Delta N\text{-}Bcat}$ mouse (hereafter referred to as "Bcat") was generated from a knockin gene targeting vector comprising a lox(P)-flanked IRES-neo cassette and a cDNA in which the FLAG-epitope tag replaced the most amino terminal 131 amino acids of mouse *β-catenin*. The IRES sequence used is a modified version of the 5'UTR from EMCV mRNA (Mountford et al., 1994). The vector (Orner et al., 2002) also contained flanking sequences homologous to the last coding exon of gpA33 and its 3'-untranslated region in order to capture all the *cis*-acting regulatory elements that collectively specify and confine expression of the resulting bicistronic RNA to the intestinal epithelium (Catimel et al., 1996; Heath et al., 1997; Johnstone et al., 2000). A lox(P)-flanked neo cassette provides a transcriptional roadblock for expression of the *ΔN-Bcat* transgene in *gpA33*^{Neo} mice. However, upon Cre-recombinase mediated excision of the neo-cassette following mating of female A33^{Neo} mice with male Cre-deleter mice, the modified *gpA33* locus of Bcat mice encodes a bicistronic RNA simultaneously encoding gpA33 and the FLAG-tagged ΔN(1-131)β-catenin (Orner et al., 2002). The 3' end of the IRES and the 5' ATG of the FLAG-tagged ΔN(1-131)β-catenin cDNA are separated by a short 13bp linker region (gcttgccacaacc). The targeting vector was electroporated into W9.5 ES cells (129X1/SvJ) and correctly targeted ES cells were injected

into blastocycsts derived from C57/Bl6 donor female mice. Chimeric male offspring were mated with C57/Bl6 female mice and once germ line transmission of the transgene was confirmed the mice were backcrossed for at least 10 generation onto C57/Bl6 background.

RNA Isolation

We isolated RNA from snap-frozen samples stored at -80°C. RNA was isolated using the Qiagen RNeasy Kit (Qiagen, Hilden, Germany) and judged RNA integrity on a denaturing formaldehyde-agarose gel. cDNA preparation was performed according to standard procedures, using RevertAid H-minus M-Mulv Reverse Transciptase, random primer and oligo dT primers (Fermentas, St. Leon-Rot, Germany).

Quantitative Real-time PCR

Quantitative Real-Time PCR was performed with the ABI PRISM 7300 detection system (Applied Biosystems, Foster City, USA) and using SYBRGreen dye. Relative RNA abundance was calculated using the ΔΔCT formula and normalized to the transcript levels of the housekeeping gene β-actin with the help of the Sequence Detection Software v.1.4 (Applied Biosystems, Foster City, USA). Assays were performed in duplicate. TaqMan primers for IL23 and IL17 were purchased from Life Technologies (Mulgrave, Australia). Primer sequences used for SybrGreen RT-qPCR were as follows:

β-actin/for: 5'- AGC CAG GTC CAG ACG CAG G - 3'

β-actin/rev: 5'- ACC CAC ACT GTG CCC ATC TAC -3'

β-catenin/for: 5'- GCT GAC CTG ATG GAG TTG GA - 3'

β-catenin/rev: 5'- GCT ACT TGC TCT TGC GTG AA - 3'

CD44/for: 5'- GTC TGC ATC GCG GTC AAT AG - 3'

CD44/rev: 5'- GGT CTC TGA TGG TTC CTT GTT C - 3'

Cmyc/for: 5'- TAG TGC TGC ATG AGG AGA CA - 3'

Cmyc/rev:	5’- GGT TTG CCT CTT CTC CAC AG - 3’
Cox2/for:	5’- ACA CAC TCT ATC ACT GGC ACC - 3’
Cox2/rev:	5’- TTC AGG GAG AAG CGT TTG C - 3’
Cryptdin1/for:	5’- AAG AGA CTA AAA CTG AGG AGC AGC - 3’
Cryptdin1/rev:	5’- CGA CAG CAG AGC GTG TA - 3’
CyclinD1/for:	5’- GCA CAA CGC ACT TTC TTT CCA - 3’
CyclinD1/rev:	5’- CGC AGG CTT GAC TCC AGA AG - 3’
ΔN-Bcat/for:	5’- GGA TTA CAA AGA CGA TGA TGA CAA GTT G - 3’
ΔN-Bcat/rev:	5’- GTC AGC TCA GGA ATT GCA CGT G - 3’
MMP7/for:	5’- GAG ATG TGA GCG CAC ATC AGT G - 3’
MMP7/rev:	5’- GAT GTA GGG GGA GAG TTT TCC AGT - 3’

Human Tissue samples

All samples were collected after prior informed written patient consent as part of a study (no. 1926/7) approved by the human ethics committee of the Klinikum rechts der Isar. Samples of histologically confirmed normal colon mucosa from resected specimen (n = 8), as well as from benign adenoma (n=9) were additionally analyzed. None of the patients received neoadjuvant treatment or suffered from a known second neoplastic disease. Tumors were classified according to the UICC/TNM system (7th edition): UICC stage I (n=11 cases), stage II (n=10), stage III (n=8), and stage IV (n=13). The median of histologically reviewed lymph nodes per case was 21 (range: 7–72). Tissues from all 42 patients, who underwent surgical resection between 1987 and 2006 at the Klinikum rechts der Isar, were obtained immediately after surgical resection. Specimens were transferred into liquid nitrogen and stored at −80°C.

Immunofluorescence on Tissue Sections

Cryosections of acetat-buffer (AlleMan Pharma GmbH, Rimbach, Germany) embedded mouse tissues were cut at 7µm thickness, air-dried and processed by routine H&E staining. Some tissue sections were fixed in 10% normal buffered formalin overnight, processed and embedded in paraffin. For immunofluorescence, sections were fixed with either 3% paraformaldehyde at room temperature for 20 minutes or with methanol at -20°C for 10 minutes. The paraformaldehyde-fixed sections were treated with 50 mmol/L NH_4Cl in PBS for 20 minutes and solubilized with 0.1% Triton X-100 for 5 minutes. Antibodies used were as follows: anti-α-catenin (Abcam, Cambridge, UK), anti-β-catenin (BD, Franklin Lakes, USA and Sigma-Aldrich, Saint Louis, USA, cat#C2206), anti-E-Cadherin (Invitrogen, Camarillo, USA, cat#13-1900, clone ECCD-2), anti-Cox2 (Santa Cruz, Heidelberg, Germany), anti-CD31 (PECAM1 Sigma-Aldrich, Munich, Germany), anti-Ki67, anti-Lysozym (Dako, Hamburg, Germany) and the dyes 4, 6- diamidino-2-phenyl indol (DAPI, Sigma, Munich, Germany), TRITC-Phalloidin (Sigma, Munich, Germany) and TRITC-UEA1 (Sigma, Munich, Germany). Immunofluorescent staining of mouse tissue sections was detected with a Zeiss Axiovert 200M microscope with an AxiocamMR3 camera, with the following objectives: LD A-Plan 10x/NA:0.25, LD A-Plan 20x/NA:0.30, Plan Neofluoar 40x/NA:0.75 lenses (all lenses: air, no immersion liquid). The tissues were imaged using standard filter sets and laser lines, acquiring single labeled images. DAPI, FITC and Cy3 fluorescence were excited with a HXP120C lamp with filters at excitation wavelengths of 360nm, 490nm, and 550nm, respectively and the emission wavelength were measured at wavelengths 460nm, 520nm, and 562nm, respectively. The images were captured using Zeiss Axiovision software (version 4.8.2). The Zeiss image files (.zvi) were imported into the Adobe Photoshop version 12.0.4 software for processing and display.

For immunofluorescence staining of paraffin embedded tissue, sections were dewaxed in xylene and rehydrated. Antigen retrieval was in boiling 10 mM citrate buffer pH 6.0 for 15 minutes. Primary antibodies were diluted in 5% normal goat serum/0.5% Triton X-100 in PBS and incubated overnight at 4°C. Secondary antibodies used were goat anti-mouse IgG, goat anti-rat IgG and goat anti-rabbit IgG coupled to Alexa488, 546 or Cy3 (Molecular Probes, Eugene, USA). Tissues were mounted in ProLong Antifade plus DAPI (Life Technologies, Mulgrave, Australia). Immunofluorescent staining of the distal colon was detected with a Leica SP8 Confocal microscope with Resonant Scanner (C4.50) on a 10x water immersion (NA 0.40) lens. The tissues were imaged using standard filter sets and laser lines, acquiring single labeled images. DAPI and □-catenin fluorescence were excited with the 405nm and 488nm laser lines, respectively and the emission wavelength were measured at wavelengths 405nm and 473nm, respectively. The images were captured using Leica's LAS-AF software. The Leica image files (lif) were imported into the ImageJ/Fiji software (Schindelin et al., 2012) for processing and display.

3D confocal fluorescence imaging

Immunofluorescent staining of crypts was detected with an Olympus FV1000 Spectral Confocal attachment to an Olympus IX-81 microscope on either a 60x water immersion (NA 1.2). The crypts were imaged using standard filter sets and laser lines, acquiring single labeled images. DAPI, β-catenin and E-cadherin fluorescence were excited with the 405nm, 488nm and 546nm laser lines, respectively and the emission wavelength were measured at wavelengths 405nm, 473nm and 559nm, respectively. The images were captured using Olympus FluoroView software (Version 1.7c). 3D image stacks were acquired, which encompass the entire depth of the crypt(s) in the field of view. The entire depth of the sample was acquired as 3D image stacks at approximately 20µm thickness for each optical section. For quantitative spatial analysis of key proteins in isolated crypts, cubic voxels were acquired

for each image stack. The output analogue signal, representing the fluorescence intensities was digitized to 16 bits resolution at 65536 levels of grey and saved as an Olympus Image Binary (OIB) image. The Olympus Image Binary (OIB) image files from the fluorescently stained individual whole mount crypts were imported into the ImageJ/Fiji software(Schindelin et al., 2012) for processing and display. 3D image stacks were extracted, and imported as „tiff" files into MATLAB (MathWorks, Natick, Massachusetts, USA), for analysis. Quantitation of β-catenin and E-cadherin was conducted as described (Tan et al., 2013).

Preparation of Protein Lysates

Protein lysates were prepared from tissue samples stored at -80°C. Samples were homogenized in a Dounce Homogenizer (Wheaton, Mellville, USA) with RIPA buffer (50 mmol/L Tris-HCl, pH 7.5, 150 mmol/L NaCl, 1 mmol/L EDTA, 1% NP-40, 0.25% sodium-deoxycholate, 0.1% SDS and protease inhibitor cocktail (Roche, Mannheim, Germany). Soluble proteins were extracted after a 15,000g centrifugation for 15 minutes at 4°C.

Immunoprecipitation and Immunoblotting

Protein G sepharose beads were incubated with 2 µg of anti-β-catenin, anti-FLAG or anti-E-cadherin antibody for 1 hour at 4°C, and 40 µl of the sepharose/antibody mixture was added to 400 µl cell lysate (see above). After 2 hours incubation the samples were centrifuged at 15,000 g for 30 seconds at 4°C and washed 3 times with RIPA buffer.

For immunoblotting, protein lysates were separated by SDS polyacrylamide gel electrophoresis under reducing conditions and transferred to a nitrocellulose membrane as described (Laemmli, 1970; Towbin et al., 1979). Immunoreactive bands were detected using anti-α-Tubulin and anti-E-Cadherin antibodies (Calbiochem, Darmstadt, Germany), anti-β-

Catenin (BD, Franklin Lakes, USA), anti-Apc (sc-896, Santa Cruz, Heidelberg, Germany), anti-FLAG (Dianova), and anti-Lamin antibodies (Cell Signaling Technology, Beverly, USA). Secondary antibodies were either horseradish peroxidase-conjugated goat anti-mouse IgG, goat anti-rabbit IgG or goat anti-rat IgG (Jackson Immunoresearch, West Grove, USA), and bands were visualized with an enhanced chemiluminescence substrate detection kit (Pierce, Rockford, USA).

Isolation of Cytosolic and Nuclear Fractions

Tissue samples were resuspended in ice-cold CLB buffer (10 mM Hepes,10 mM NaCl, 5 mM $NaHCO_3$, 1 mM $CaCl_2$, 0,5 mM MgCl2, 5 mM EDTA,1 mM Pefablock and protease inhibitor cocktail) on ice for 5 minutes, homogenized in a Dounce Homogenizer (Wheaton, Mellville, USA) and centrifuged at 3000 rpm (4°C) for 5 minutes. The cytosolic fraction (supernatant) was harvested after a centrifugation at 39,000 g for 15 minutes. The nuclear fraction (pellet) was resuspended in TSE buffer (10 mM Tris/HCl ph 7.5, 0.3 M Sucrose, 1 mM EDTA, 0.1% NP-40, 1 mM Pefablock and protease inhibitor cocktail), homogenized and centrifuged at 3000 rpm (4°C) for 5 minutes. The pellet was resuspended in 100 µl RIPA buffer (see above), and the samples were prepared for immunoblotting or immunoprecipitation.

Tumor Analysis and Processing of Tissue

Intestines were collected from mice at the indicated age and opened longitudinally, to determine the size and location of macroscopically visible tumors, prior to their resection and embedding in acetate-buffer (sodium acetate, sodium chloride, potassium chloride, calcium chloride, magnesium chloride hexahydrate, with respective molarities: 140 mmol/l Na+, 4 mmol/l K+, 2.5 mmol/l Ca2+, 1 mmol/l Mg2+, 106 mmol/l Cl-, 45 mmol/l acetate, pH: 6.7-7.7 (AlleMan Pharma GmbH, Rimbach, Germany)) and processing for cryosections. Some freshly isolated tumors were snap-frozen in liquid nitrogen and stored at -80°C for subsequent

DNA/RNA extraction or protein analysis. Aberrant crypt foci (ACF) in the colonic mucosa of longitudinally opened, pinned out and fixed tissues (over night in 75% ethyl alcohol, 20% formaldehyde and 5% acetic acid) were detected after staining for 1 minute in 0.2% methylene blue (Sigma, Munich, Germany) in PBS and rinsed in fresh phosphate buffer at 4°C for 2 hours. The tissue segments were placed with the luminal side up on microscope slides and observed with a low-magnification lens. All ACFs were at least 3 times larger in diameter than normal crypts, and their lumina were mostly oval or elongated rather than circular (McLellan and Bird, 1988).

Azoxymethane (AOM)-induced mutagenesis

Eight week old mice were injected with 10 mg/kg AOM intraperitoneally once weekly for 6 consecutive weeks. Colons were collected either 5 weeks after the last AOM challenge to assess for ACF, or at 12 weeks to assess for colonic adenomas. We used Sanger sequencing on genomic DNA prepared from adenomas to assess for AOM-induced amino acid substitution mutation K-ras (G12, G13, Q61) and β-catenin (S37, S38). Loss-of-heterozygosity was implicated by immunohistochemical absence of Apc protein staining using an antibody raised against the C-terminus of APC (sc-896, Santa Cruz, Heidelberg, Germany).

TRITC-dextran permeability assay

Intestinal permeability was assessed by gastric gavage of TRITC-dextran (40 mg/ml, 4 kDa in PBS; Sigma, Munich, Germany) as a non-metabolizable macromolecule(Brandl et al., 2009). Prior to the TRITC-dextran challenge (200 □l of a 40 mg/ml solution), we sensitized mice by providing 2% DSS in drinking for 16 hours. TRITC-dextran measurements in plasma were performed 4 hours after the challenge using fluorometry.

Statistics

Unless otherwise indicated, Student's t-test were performed and data expressed as means $\pm$ s.e.m.

Acknowledgments

The work in the laboratory of ME is supported by the Ludwig Institute for Cancer Research, the Victorian State Government Operational Infrastructure Support, the IRIISS scheme of the National Health and Medical Research Council Australia (NHMRC), and NHMRC grants #487922, #433617, #603122 and #1064987 (to MB and ME). ME is an NHMRC Senior Research Fellow.

RHD is supported by NIH P01 grant CA090890 and a Chancellor's Research Initiative from Texas A&M.

Work in the laboratory of K-PJ is supported by grants from the Wilhelm-Sander Stiftung, the KKF (Kommission fuer klinische Forschung, Medical Faculty, TUM), and by a grant from DAAD/INCA Joint Translational Research Program on Cancer (to GO and K-PJ).

The authors thank the staff of the animal house, histology and microscopy facilities at TUM and WEHI for expert technical assistance.

Competing interests

Authors have nothing to disclose

Author contributions

KPJ, ME, JKH, RHD - Study concept and design

MB, FR, ME, NT, BW, CWT, YH, GO, AG, AO, GO - Acquisition, analysis and interpretation of data

MB, BW, CWT, ME, FR, GO - Statistical analysis

MB, KPJ - Drafting of manuscript

ME, KPJ, RHD - Critical revision of the manuscript

Funding

Wilhelm Sander-Stiftung and KKF (Kommission fuer Klinische Forschung, Medical Faculty, TUM) to KPJ, DAAD/INCA (to GO and KPJ), NHMRC (grants #487922, #433617, #603122 (to ME) and #1064987 (to MB and ME))

REFERENCES

Albuquerque, C., Baltazar, C., Filipe, B., Penha, F., Pereira, T., Smits, R., Cravo, M., Lage, P., Fidalgo, P., Claro, I. et al. (2010). Colorectal cancers show distinct mutation spectra in members of the canonical WNT signaling pathway according to their anatomical location and type of genetic instability. *Genes Chromosomes Cancer* **49**, 746-59.

Andreu, P., Peignon, G., Slomianny, C., Taketo, M. M., Colnot, S., Robine, S., Lamarque, D., Laurent-Puig, P., Perret, C. and Romagnolo, B. (2008). A genetic study of the role of the Wnt/beta-catenin signalling in Paneth cell differentiation. *Dev Biol* **324**, 288-96.

Araki, Y., Okamura, S., Hussain, S. P., Nagashima, M., He, P., Shiseki, M., Miura, K. and Harris, C. C. (2003). Regulation of cyclooxygenase-2 expression by the Wnt and ras pathways. *Cancer Res* **63**, 728-34.

Barker, N., Ridgway, R. A., van Es, J. H., van de Wetering, M., Begthel, H., van den Born, M., Danenberg, E., Clarke, A. R., Sansom, O. J. and Clevers, H. (2009). Crypt stem cells as the cells-of-origin of intestinal cancer. *Nature* **457**, 608-11.

Benary, U., Kofahl, B., Hecht, A. and Wolf, J. (2013). Modeling Wnt/beta-Catenin Target Gene Expression in APC and Wnt Gradients Under Wild Type and Mutant Conditions. *Front Physiol* **4**, 21.

Brandl, K., Rutschmann, S., Li, X., Du, X., Xiao, N., Schnabl, B., Brenner, D. A. and Beutler, B. (2009). Enhanced sensitivity to DSS colitis caused by a hypomorphic Mbtps1 mutation disrupting the ATF6-driven unfolded protein response. *Proc Natl Acad Sci U S A* **106**, 3300-5.

Bochkov, Y. A. and Palmenberg, A. C. (2006). Translational efficiency of EMCV IRES in bicistronic vectors is dependent upon IRES sequence and gene location. *Biotechniques* **41**, 283-4, 286, 288 passim.

Buchert, M., Athineos, D., Abud, H. E., Burke, Z. D., Faux, M. C., Samuel, M. S., Jarnicki, A. G., Winbanks, C. E., Newton, I. P., Meniel, V. S. et al. (2010). Genetic dissection of differential signaling threshold requirements for the Wnt/beta-catenin pathway *in vivo*. *PLoS Genet* **6**, e1000816.

Catimel, B., Ritter, G., Welt, S., Old, L. J., Cohen, L., Nerrie, M. A., White, S. J., Heath, J. K., Demediuk, B., Domagala, T. et al. (1996). Purification and characterization of a novel restricted antigen expressed by normal and transformed human colonic epithelium. *J Biol Chem* **271**, 25664-70.

Claessen, M. M., Schipper, M. E., Oldenburg, B., Siersema, P. D., Offerhaus, G. J. and Vleggaar, F. P. (2010). WNT-pathway activation in IBD-associated colorectal carcinogenesis: potential biomarkers for colonic surveillance. *Cell Oncol* **32**, 303-10.

Clevers, H. (2006). Colon cancer--understanding how NSAIDs work. *N Engl J Med* **354**, 761-3.

Darken, R. S. and Wilson, P. A. (2001). Axis induction by wnt signaling: Target promoter responsiveness regulates competence. *Dev Biol* **234**, 42-54.

Dikovskaya, D., Schiffmann, D., Newton, I. P., Oakley, A., Kroboth, K., Sansom, O., Jamieson, T. J., Meniel, V., Clarke, A. and Nathke, I. S. (2007). Loss of APC induces polyploidy as a result of a combination of defects in mitosis and apoptosis. *J Cell Biol* **176**, 183-95.

Dimberg, J., Hong, T. T., Skarstedt, M., Lofgren, S., Zar, N. and Matussek, A. (2013). Analysis of APC and IGFBP7 promoter gene methylation in Swedish and Vietnamese colorectal cancer patients. *Oncol Lett* **5**, 25-30.

Fodde, R., Edelmann, W., Yang, K., van Leeuwen, C., Carlson, C., Renault, B., Breukel, C., Alt, E., Lipkin, M., Khan, P. M. et al. (1994). A targeted chain-termination

mutation in the mouse Apc gene results in multiple intestinal tumors. *Proc Natl Acad Sci U S A* **91**, 8969-73.

Gay, L. J., Mitrou, P. N., Keen, J., Bowman, R., Naguib, A., Cooke, J., Kuhnle, G. G., Burns, P. A., Luben, R., Lentjes, M. et al. (2012). Dietary, lifestyle and clinicopathological factors associated with APC mutations and promoter methylation in colorectal cancers from the EPIC-Norfolk study. *J Pathol* **228**, 405-15.

Grivennikov, S. I., Wang, K., Mucida, D., Stewart, C. A., Schnabl, B., Jauch, D., Taniguchi, K., Yu, G. Y., Osterreicher, C. H., Hung, K. E. et al. (2012). Adenoma-linked barrier defects and microbial products drive IL-23/IL-17-mediated tumour growth. *Nature* **491**, 254-8.

Hanson, C. A. and Miller, J. R. (2005). Non-traditional roles for the Adenomatous Polyposis Coli (APC) tumor suppressor protein. *Gene* **361**, 1-12.

Harada, N., Tamai, Y., Ishikawa, T., Sauer, B., Takaku, K., Oshima, M. and Taketo, M. M. (1999). Intestinal polyposis in mice with a dominant stable mutation of the beta-catenin gene. *EMBO J* **18**, 5931-42.

Heath, J. K., White, S. J., Johnstone, C. N., Catimel, B., Simpson, R. J., Moritz, R. L., Tu, G. F., Ji, H., Whitehead, R. H., Groenen, L. C. et al. (1997). The human A33 antigen is a transmembrane glycoprotein and a novel member of the immunoglobulin superfamily. *Proc Natl Acad Sci U S A* **94**, 469-74.

Janssen, K. P., Alberici, P., Fsihi, H., Gaspar, C., Breukel, C., Franken, P., Rosty, C., Abal, M., El Marjou, F., Smits, R. et al. (2006). APC and oncogenic KRAS are synergistic in enhancing Wnt signaling in intestinal tumor formation and progression. *Gastroenterology* **131**, 1096-109.

Jarde, T., Evans, R. J., McQuillan, K. L., Parry, L., Feng, G. J., Alvares, B., Clarke, A. R. and Dale, T. C. (2013). *In vivo* and *in vitro* models for the therapeutic targeting of Wnt signaling using a Tet-ODeltaN89beta-catenin system. *Oncogene* **32**, 883-93.

Jen, J., Powell, S. M., Papadopoulos, N., Smith, K. J., Hamilton, S. R., Vogelstein, B. and Kinzler, K. W. (1994). Molecular determinants of dysplasia in colorectal lesions. *Cancer Res* **54**, 5523-6.

Johnstone, C. N., Tebbutt, N. C., Abud, H. E., White, S. J., Stenvers, K. L., Hall, N. E., Cody, S. H., Whitehead, R. H., Catimel, B., Nice, E. C. et al. (2000). Characterization of mouse A33 antigen, a definitive marker for basolateral surfaces of intestinal epithelial cells. *Am J Physiol Gastrointest Liver Physiol* **279**, G500-10.

Joo, M., Shahsafaei, A. and Odze, R. D. (2009). Paneth cell differentiation in colonic epithelial neoplasms: evidence for the role of the Apc/beta-catenin/Tcf pathway. *Hum Pathol* **40**, 872-80.

Laemmli, U. K. (1970). Cleavage of structural proteins during the assembly of the head of bacteriophage T4. *Nature* **227**, 680-5.

Leedham, S. J., Rodenas-Cuadrado, P., Howarth, K., Lewis, A., Mallappa, S., Segditsas, S., Davis, H., Jeffery, R., Rodriguez-Justo, M., Keshav, S. et al. (2013). A basal gradient of Wnt and stem-cell number influences regional tumour distribution in human and mouse intestinal tracts. *Gut* **62**, 83-93.

Lilien, J. and Balsamo, J. (2005). The regulation of cadherin-mediated adhesion by tyrosine phosphorylation/dephosphorylation of beta-catenin. *Curr Opin Cell Biol* **17**, 459-65.

Luo, F., Brooks, D. G., Ye, H., Hamoudi, R., Poulogiannis, G., Patek, C. E., Winton, D. J. and Arends, M. J. (2009). Mutated K-ras(Asp12) promotes tumourigenesis in Apc(Min) mice more in the large than the small intestines, with synergistic effects between K-ras and Wnt pathways. *Int J Exp Pathol* **90**, 558-74.

Luongo, C., Moser, A. R., Gledhill, S. and Dove, W. F. (1994). Loss of Apc+ in intestinal adenomas from Min mice. *Cancer Res* **54**, 5947-52.

McLellan, E. A. and Bird, R. P. (1988). Aberrant crypts: potential preneoplastic lesions in the murine colon. *Cancer Res* **48**, 6187-92.

Mitra, A., Menezes, M. E., Pannell, L. K., Mulekar, M. S., Honkanen, R. E., Shevde, L. A. and Samant, R. S. (2012). DNAJB6 chaperones PP2A mediated dephosphorylation of GSK3beta to downregulate beta-catenin transcription target, osteopontin. *Oncogene* **31**, 4472-83.

Mountford, P., Zevnik, B., Duwel, A., Nichols, J., Li, M., Dani, C., Robertson, M., Chambers, I. and Smith, A. (1994). Dicistronic targeting constructs: reporters and modifiers of mammalian gene expression. *Proc Natl Acad Sci U S A* **91**, 4303-7.

Orner, G. A., Dashwood, W. M., Blum, C. A., Diaz, G. D., Li, Q., Al-Fageeh, M., Tebbutt, N., Heath, J. K., Ernst, M. and Dashwood, R. H. (2002). Response of Apc(min) and A33 (delta N beta-cat) mutant mice to treatment with tea, sulindac, and 2-amino-1-methyl-6-phenylimidazo[4,5-b]pyridine (PhIP). *Mutat Res* **506-507**, 121-7.

Oyama, T., Kanai, Y., Ochiai, A., Akimoto, S., Oda, T., Yanagihara, K., Nagafuchi, A., Tsukita, S., Shibamoto, S., Ito, F. et al. (1994). A truncated beta-catenin disrupts the interaction between E-cadherin and alpha-catenin: a cause of loss of intercellular adhesiveness in human cancer cell lines. *Cancer Res* **54**, 6282-7.

Polakis, P. (1997). The adenomatous polyposis coli (APC) tumor suppressor. *Biochim Biophys Acta* **1332**, F127-47.

Polakis, P. (2000). Wnt signaling and cancer. *Genes Dev* **14**, 1837-51.

Powell, S. M., Zilz, N., Beazer-Barclay, Y., Bryan, T. M., Hamilton, S. R., Thibodeau, S. N., Vogelstein, B. and Kinzler, K. W. (1992). APC mutations occur early during colorectal tumorigenesis. *Nature* **359**, 235-7.

Pryczynicz, A., Gryko, M., Niewiarowska, K., Dymicka-Piekarska, V., Ustymowicz, M., Hawryluk, M., Cepowicz, D., Borsuk, A., Kemona, A., Famulski, W. et al. (2013). Immunohistochemical expression of MMP-7 protein and its serum level in colorectal cancer. *Folia Histochem Cytobiol* **51**, 206-12.

Qiu, Y., Fu, X., Zhang, W., Xu, Y., Xiao, L., Chen, X., Shi, L., Zhou, X., Xia, G., Peng, Y. et al. (2014). Prevalence and molecular characterisation of the sessile serrated adenoma in a subset of the Chinese population. *J Clin Pathol* **67**, 491-8.

Romagnolo, B., Berrebi, D., Saadi-Keddoucci, S., Porteu, A., Pichard, A. L., Peuchmaur, M., Vandewalle, A., Kahn, A. and Perret, C. (1999). Intestinal dysplasia and adenoma in transgenic mice after overexpression of an activated beta-catenin. *Cancer Res* **59**, 3875-9.

Roose, J., Huls, G., van Beest, M., Moerer, P., van der Horn, K., Goldschmeding, R., Logtenberg, T. and Clevers, H. (1999). Synergy between tumor suppressor APC and the beta-catenin-Tcf4 target Tcf1. *Science* **285**, 1923-6.

Samuel, M. S., Suzuki, H., Buchert, M., Putoczki, T. L., Tebbutt, N. C., Lundgren-May, T., Christou, A., Inglese, M., Toyota, M., Heath, J. K. et al. (2009). Elevated Dnmt3a activity promotes polyposis in Apc(Min) mice by relaxing extracellular restraints on Wnt signaling. *Gastroenterology* **137**, 902-13, 913 e1-11.

Sansom, O. J., Meniel, V., Wilkins, J. A., Cole, A. M., Oien, K. A., Marsh, V., Jamieson, T. J., Guerra, C., Ashton, G. H., Barbacid, M. et al. (2006). Loss of Apc allows phenotypic manifestation of the transforming properties of an endogenous K-ras oncogene *in vivo*. *Proc Natl Acad Sci U S A* **103**, 14122-7.

Sansom, O. J., Meniel, V. S., Muncan, V., Phesse, T. J., Wilkins, J. A., Reed, K. R., Vass, J. K., Athineos, D., Clevers, H. and Clarke, A. R. (2007). Myc deletion rescues Apc deficiency in the small intestine. *Nature* **446**, 676-9.

Smith, A. J., Stern, H. S., Penner, M., Hay, K., Mitri, A., Bapat, B. V. and Gallinger, S. (1994). Somatic APC and K-ras codon 12 mutations in aberrant crypt foci from human colons. *Cancer Res* **54**, 5527-30.

Smits, R., van der Houven van Oordt, W., Luz, A., Zurcher, C., Jagmohan-Changur, S., Breukel, C., Khan, P. M. and Fodde, R. (1998). Apc1638N: a mouse model for familial adenomatous polyposis-associated desmoid tumors and cutaneous cysts. *Gastroenterology* **114**, 275-83.

Su, L. K., Kinzler, K. W., Vogelstein, B., Preisinger, A. C., Moser, A. R., Luongo, C., Gould, K. A. and Dove, W. F. (1992). Multiple intestinal neoplasia caused by a mutation in the murine homolog of the APC gene. *Science* **256**, 668-70.

Takeda, A., Otani, Y., Iseki, H., Takeuchi, H., Aikawa, K., Tabuchi, S., Shinozuka, N., Saeki, T., Okazaki, Y. and Koyama, I. (2007). Clinical significance of large tenascin-C spliced variant as a potential biomarker for colorectal cancer. *World J Surg* **31**, 388-94.

Tan, C. W., Hirokawa, Y., Gardiner, B. S., Smith, D. W. and Burgess, A. W. (2013). Colon cryptogenesis: asymmetric budding. *PLoS One* **8**, e78519.

Towbin, H., Staehelin, T. and Gordon, J. (1979). Electrophoretic transfer of proteins from polyacrylamide gels to nitrocellulose sheets: procedure and some applications. *Proc Natl Acad Sci U S A* **76**, 4350-4.

van Dekken, H., Wink, J. C., Vissers, K. J., Franken, P. F., Ruud Schouten, W., WC, J. H., Kuipers, E. J., Fodde, R. and Janneke van der Woude, C. (2007). Wnt pathway-related gene expression during malignant progression in ulcerative colitis. *Acta Histochem* **109**, 266-72.

van Es, J. H., Jay, P., Gregorieff, A., van Gijn, M. E., Jonkheer, S., Hatzis, P., Thiele, A., van den Born, M., Begthel, H., Brabletz, T. et al. (2005). Wnt signalling induces maturation of Paneth cells in intestinal crypts. *Nat Cell Biol* **7**, 381-6.

Wang, D., Mann, J. R. and DuBois, R. N. (2005). The role of prostaglandins and other eicosanoids in the gastrointestinal tract. *Gastroenterology* **128**, 1445-61.

Wong, M. H., Rubinfeld, B. and Gordon, J. I. (1998). Effects of forced expression of an NH2-terminal truncated beta-Catenin on mouse intestinal epithelial homeostasis. *J Cell Biol* **141**, 765-77.

Xia, D., Wang, D., Kim, S. H., Katoh, H. and DuBois, R. N. (2012). Prostaglandin E2 promotes intestinal tumor growth via DNA methylation. *Nat Med* **18**, 224-6.

Figures

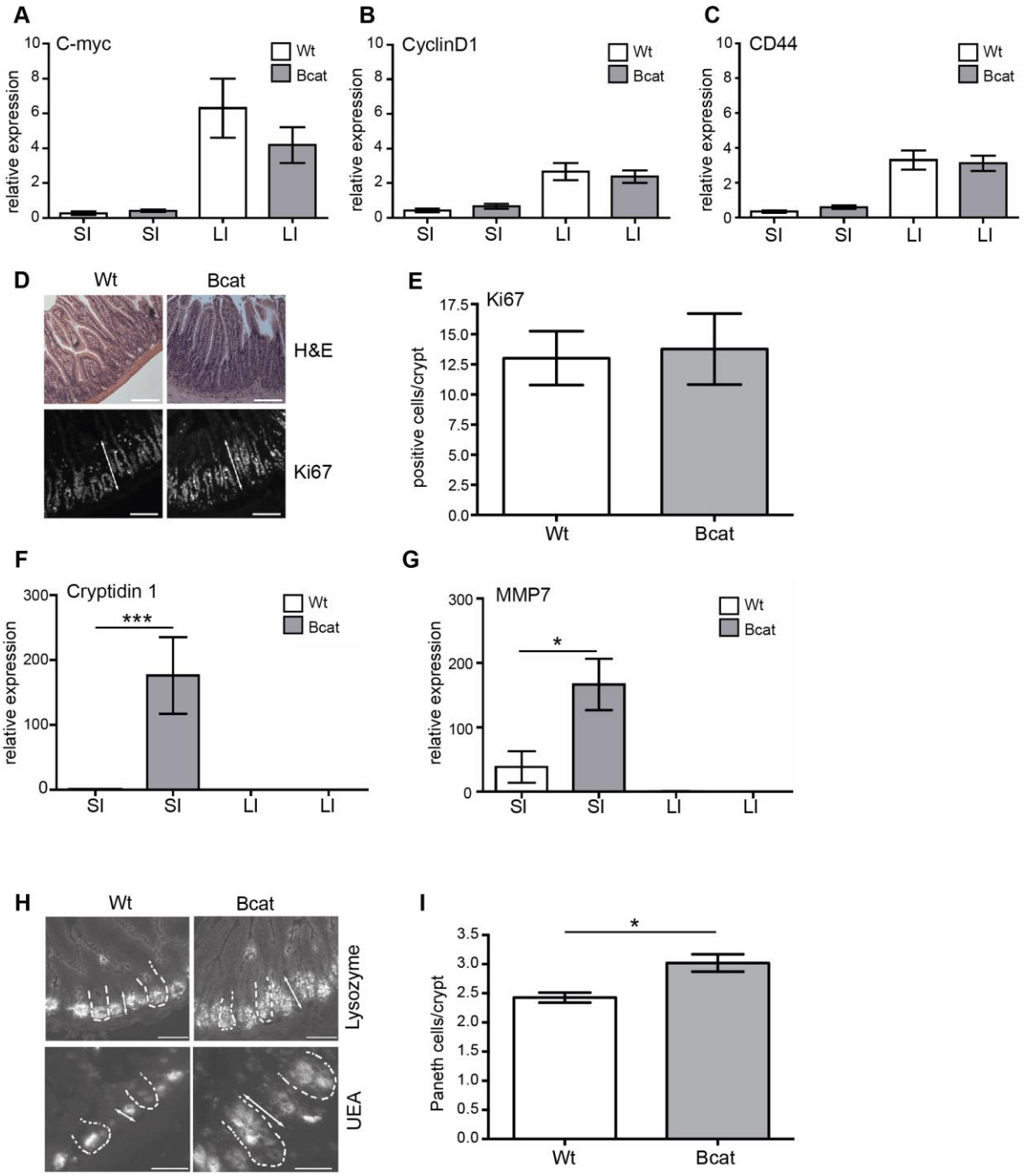

Figure 1 Only some Wnt target genes are induced in pre-malignant intestinal tissue of Bcat mice.

(A-C) mRNA expression determined by quantitative real-time PCR in small (SI) and large (LI) intestine from wild type (Wt) (n=5) and Bcat (n=12) mice. Expression was normalized to the median expression of all wild type SI and LI samples, respectively. All measurements were done in duplicate.

(D) Hematoxylin and eosin (H&E) and Ki67 stain of small intestine from Wt and Bcat mice (100x magnification, scale bar = 100 μm).

(E) Quantitation of Ki67 positive cells in the intestine of Wt and Bcat mice and normalized per fully visible crypt.

(F,G) Cryptdin 1 and MMP7 mRNA expression in the SI and LI of Wt and Bcat mice. mRNA expression is increased in SI in Bcat mice in comparison to Wt mice but absent in the large intestine. (* $P< 0.05$; *** $P< 0.001$)

(H) Staining for Lysozyme (100x magnification, scale bar = 100 μm) and Ulex Europaeus Agglutinin lectin (UEA, 200x magnification, scale bar = 50 μm) in the SI of Wt and Bcat mice. The dashed lines indicate the outline of individual intestinal crypts.

(I) Quantitation of Paneth cells in the SI of Wt and Bcat mice (* $p<0.05$, n = 3 mice per genotype, 20 fully visible crypts per mouse were counted).

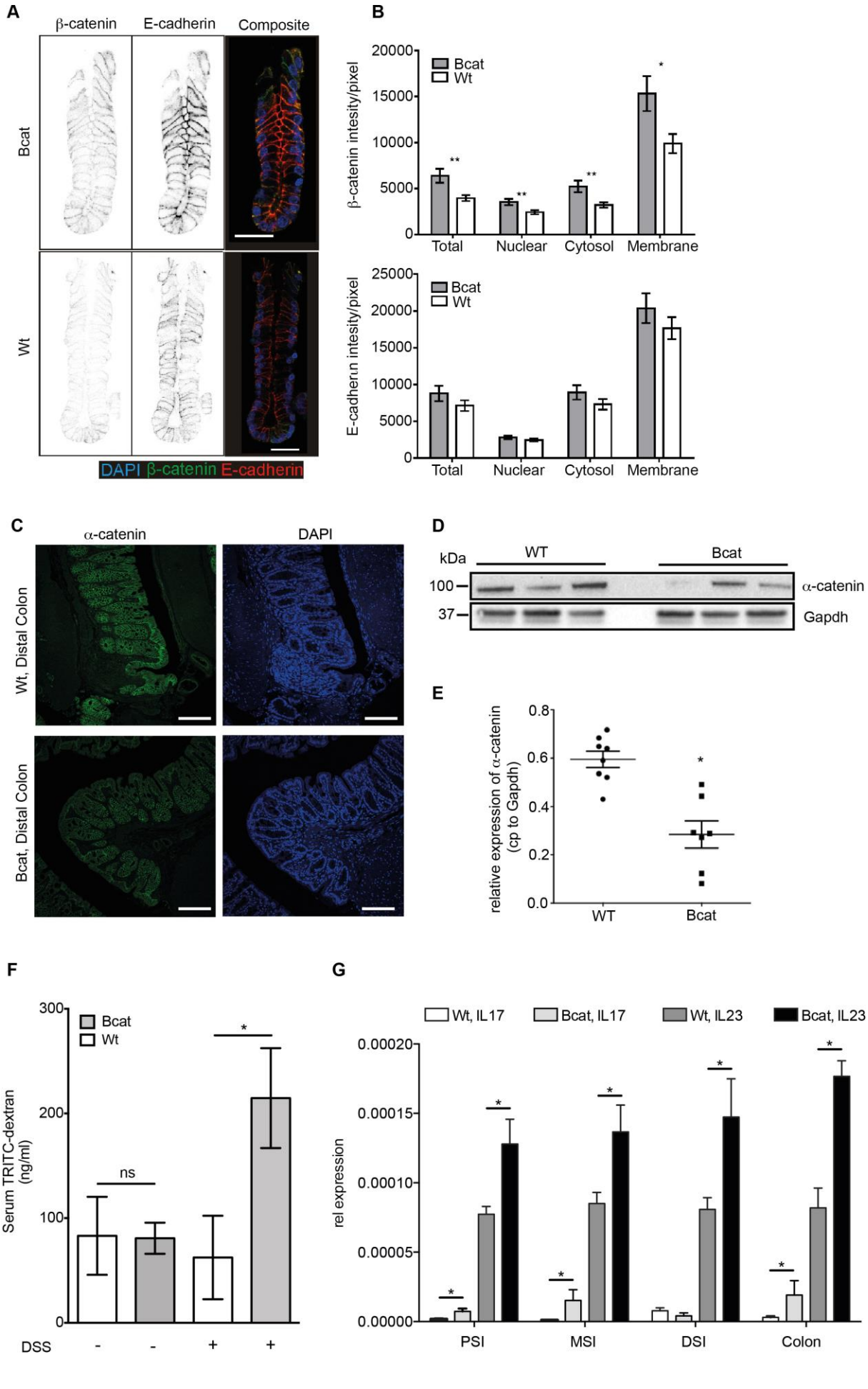

Figure 2 Intestinal permeability defect in Bcat mice is associated with mislocalization of membrane-associated proteins.

(A) β-catenin and E-cadherin staining on isolated colonic crypts from Bcat and wild type (Wt) mice. In the composite image β-catenin is stained in green, E-cadherin in red and DAPI labelled cell nuclei are blue (scale bar = 30 μm).

(B) Quantitation of staining intensity of β-catenin (top panel) and E-cadherin (bottom panel) in the indicated subcellular compartments (* $p<0.05$, ** $p<0.01$, single factor anova analysis, n=15 Bcat and n=24 Wt mice).

(C) Confocal immunofluorescence images of α-catenin (green) in distal colon of Bcat and Wt mice. DAPI (blue) labels nuclei. (scale bar = 100 μm).

(D) Western blot analysis of α-catenin protein expression in colonic shakepreps of Wt and Bcat mice. Shown is a representative Western blot of 1 of three independent experiments. Each lane represents one mouse. Gapdh was used as loading control.

(E) Scatter plot showing the expression levels of α-catenin protein normalised to Gapdh in colonic shakepreps of Wt and Bcat mice (* $p<0.05$; n=9 mice per genotype).

(F) Intestinal permeability determined by the absorbance of TRITC-dextran in the serum 4 hours after oral gavage of TRITC-dextran (4 kDa) in Wt and Bcat mice. A cohort of mice was also challenged by 2% DSS in the drinking water for 16 hours prior to the TRITC-dextran gavage (* $p<0.05$, n=5-8 mice per genotype**)**.

(G) mRNA expression of IL-17 and IL-23 cytokines in proximal, middle and distal small intestine as well as colon of Wt and Bcat mice (* $p<0.05$, n=3 mice per genotype).

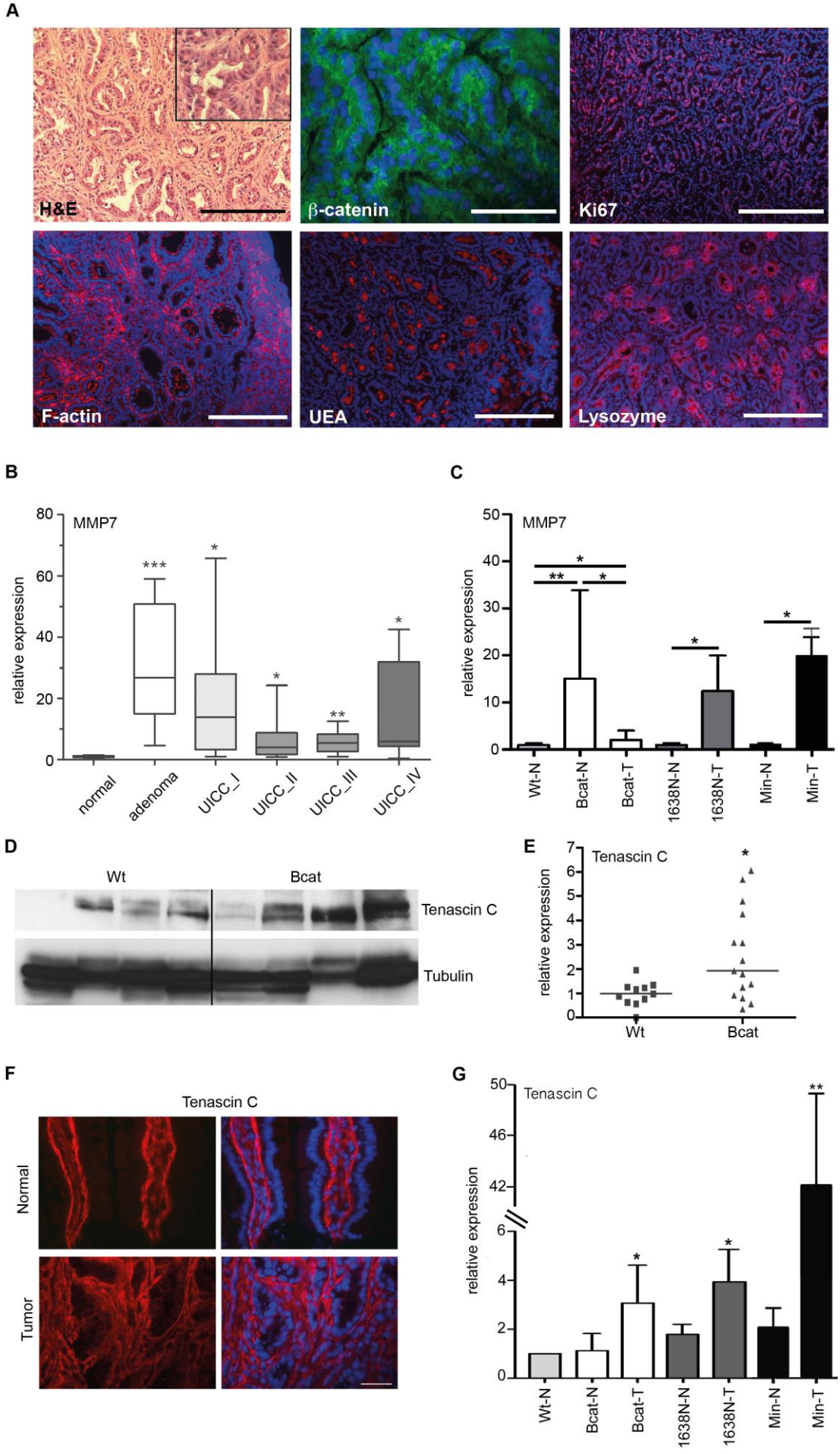

Figure 3 MMP7 is upregulated in normal epithelium of Bcat mice and early stage human colon cancer.

(A) Spontaneously arising tumors in the small intestine of Bcat mice show well differentiated to high-grade adenoma (50x magnification, scale bar = 200 µm, inset: 200x magnification). Immunofluorescence staining for β-catenin, proliferation marker Ki67, F-actin (TRITC-Phalloidin), and the Paneth cell markers UEA and Lysozyme. Cell nuclei are stained blue with DAPI. (β-catenin: 400x magnification, scale bar = 25 µm; all others: 100x magnification, scale bar = 100 µm).

(B) MMP7 RNA expression in human colon cancer specimen in normal mucosa (n=8), benign adenomas (n=9), locally restricted early stage carcinoma (UICC I; n=11), carcinoma UICC stage II (n=10), carcinoma UICC stage III (n=8), and carcinoma UICC stage IV (n=13). The qRT-PCR data were normalized to expression of HPRT (* $p<0.05$, ** $p<0.01$, *** $p<0.001$; unpaired student's t-test).

(C) RT-qPCR analysis of MMP7 expression in normal (N) and tumor (T) tissue from mice of the indicated genotypes (* $p<0.05$, ** $p<0.01$, $n\geq3$, student's t-test)

(D,E) Western blot analysis and associated quantitation of Tenascin-C protein expression in non-neoplastic small intestine of Wt and Bcat mice. Each lane represents one mouse (* $p<0.05$; n=4 mice per genotype).

(F) Immunofluorescence staining with a specific anti-Tenascin-C antibody in normal and tumoral intestine of Bcat mice. Cell nuclei are stained blue with DAPI. (100x magnification, scale bar = 100 µm).

(G) RT-qPCR analysis of Tenascin-C expression in normal (N) and tumor (T) tissue from mice of the indicated genotypes (* $p<0.05$, ** $p<0.01$, $n\geq3$, student's t-test)

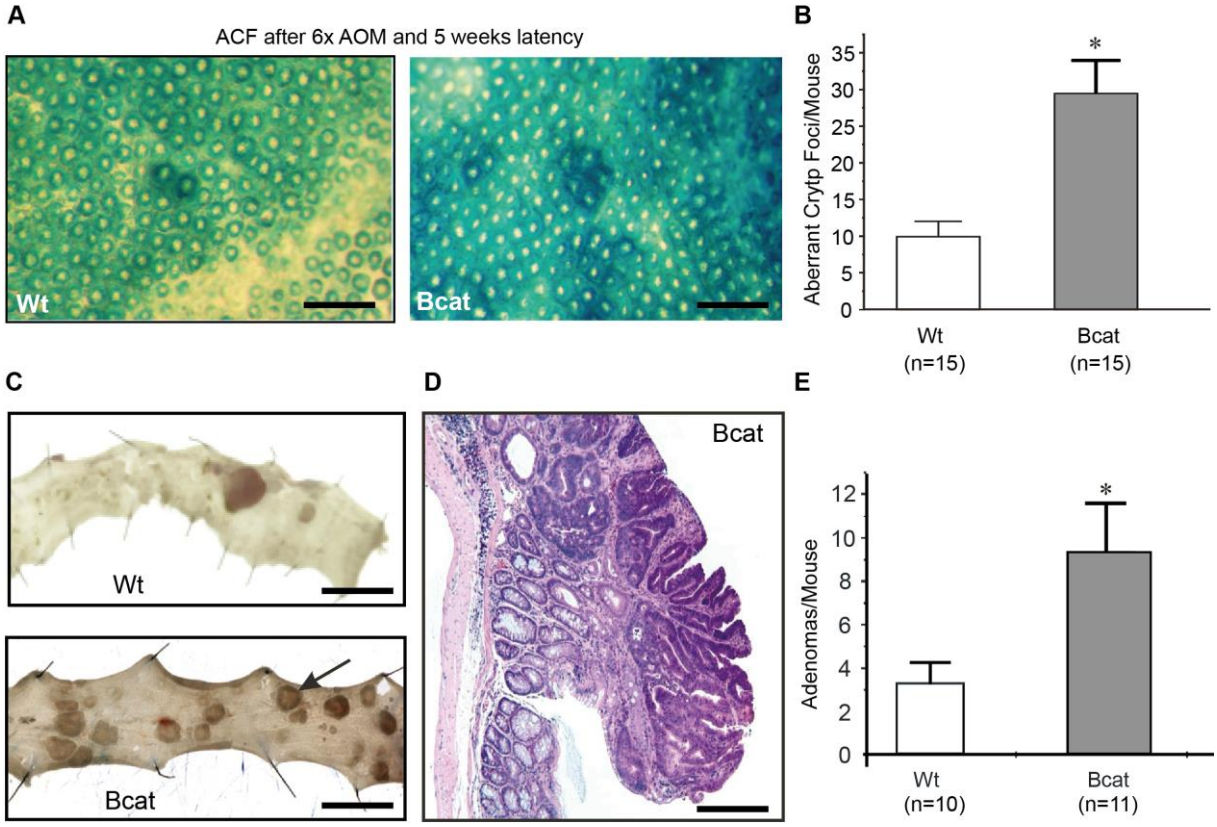

Figure 4 The intestinal epithelium of Bcat mice has increased susceptibility to mutagen-induced carcinogenesis.

(A) Representative methylene blue stained large intestine of wild type (Wt) and Bcat mice 5 weeks after last of 6 consecutive azoxymethane (AOM) injections (scale bar = 400 μm).

(B) Enumeration of aberrant crypt foci in the colonic epithelium of Wt and Bcat mice. (mean ± s.d, n=15 mice, * $p<0.05$).

(C) Photomicrographs of longitudinally opened and pinned out colons from Wt and Bcat mice 16 weeks after last injection of AOM (scale bar = 1 cm).

(D) H&E stain of a representative colonic adenoma excised from a Bcat mouse 16 weeks after the last AOM in injection (scale bar = 20 μm).

(E) Enumeration of macroscopically visible adenomas in AOM-challenged Wt and Bcat mice (mean ± s.d, n=10-11 mice, * $p<0.05$)

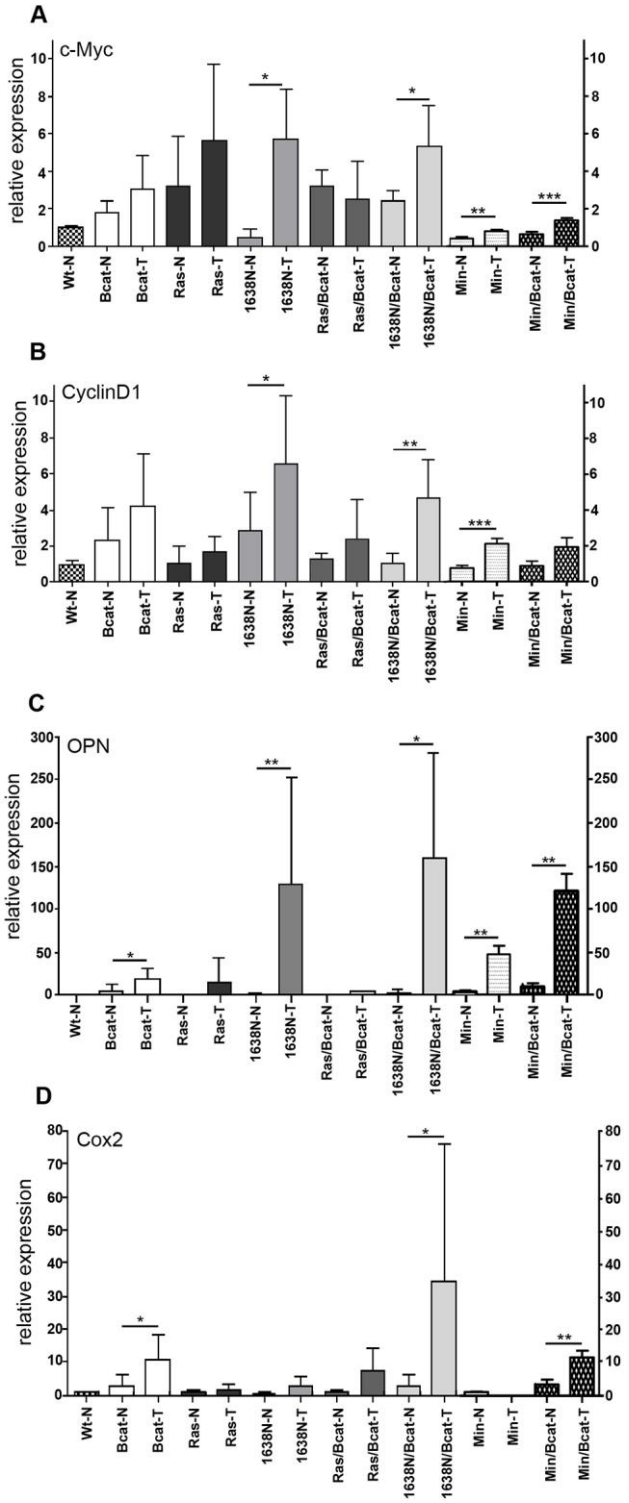

Figure 5 Regulation of selected Wnt target genes in tumors of mice of the indicated genotype where no difference in proliferation is detected upon expression of the □N-Bcat transgene (data not shown).

(A,B) RT-qPCR analysis of c-Myc and cyclinD1 expression in normal (N) and tumor (T) tissue from mice of the indicated genotypes (* $p<0.05$, ** $p<0.01$, *** $P<0.001$; $n\geq5$ tumors).

(C,D) RT-qPCR analysis of osteopontin (OPN) and cyclooxygenase 2 (Cox2) expression in normal (N) and tumor (T) tissue from mice of the indicated genotypes (* $p<0.05$, ** $p<0.01$, *** $P<0.001$; $n\geq5$ tumors).

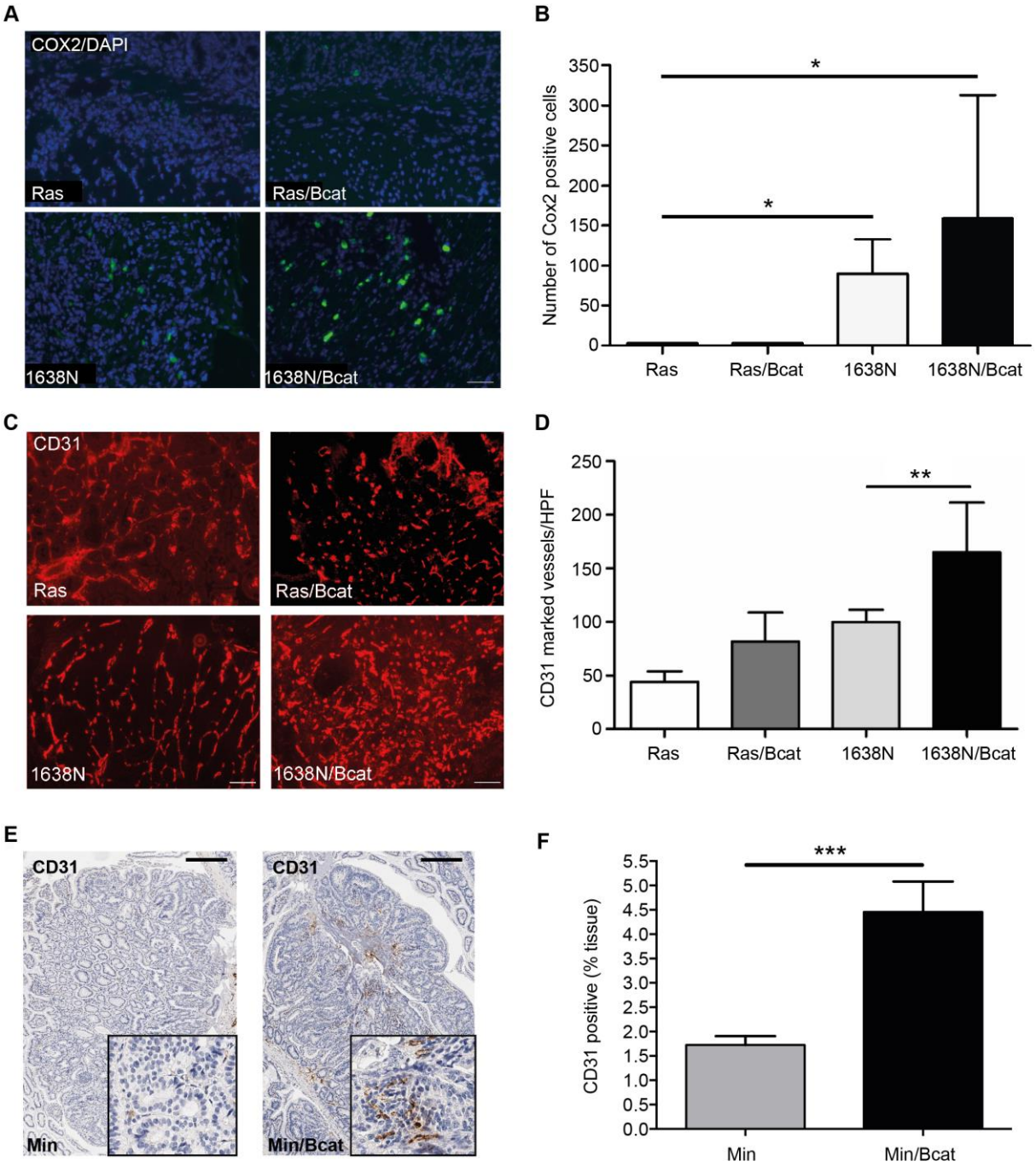

Figure 6 Increased tumor angiogenesis in Bcat mice.

(A) Representative immunohistochemical Cox2 staining of tumor sections of the indicated genotypes (100x magnification, scale bar = 100 μm).

(B) Enumeration of Cox2 positive cells per high-power field (HPF) of view in tumor sections from mice of the indicated genotypes. (*$p<0.05$; 10 HPFs counted per mouse and $n>3$ mice per genotype)

(C) Immunofluorescence of cryosections stained with anti-CD31 antibody on tumors from mice of the indicated genotypes (100x magnification, scale bar = 100 μm).

(D) Quantitation of CD31 stained positive vessels per HPF (** $p<0.01$; 10 HPFs counted per mouse and $n>3$ mice per genotype).

(E) Representative immunohistochemical CD31 staining of cells in intestinal tissue sections of Min and Min/Bcat mice. (20x magnification, scale bar = 100 μm, tumor inset: 200x magnification)

(F) Quantitation of CD31 stained area in tumours from Min and Min/Bcat mice (*** $p<0.001$, $n=3$ mice per genotype).

Tables

Table 1: Incidence, size and distribution of tumors from different mouse models of colorectal cancer.

Genotype	Number of mice	Age (months)	Tumors per animal	Incidence	Avg size of tumors (SD, mm)	Localisation of tumors			
						PSI	MSI	DSI	Colon
Ras	57	17	2.3	56%	2.0±0.9	37%	43%	20%	0%
Bcat	54	17	1.7	37%	2.2±1.7	10%	25%	5%	60%
1638N	60	9	3.9	95%	3.4±1.8	66%	27%	5%	2%
Min	4	8	22.3	100%	2.5±1.5	50%	23%	23%	4%
Ras/Bcat	14	17	4.0	64%	2.0±1.2	47%	31%	19%	3%
1638N/Bcat	8	7	7.8	100%	3.1±1.9	53%	34%	10%	3%
Min/Bcat	5	8	62.5	100%	2.7±1.5	23%	28%	40%	9%

Mice carrying the indicated mutant alleles were harvested at the indicated time. The incidence, number, size and localisation of intestinal tumors were determined.

TRANSLATIONAL IMPACT

Clinical issue

Colon cancer is the second leading cause of cancer mortality in many industrialized countries. Activation of the Wnt/β-catenin pathway occurs in a vast majority of colorectal cancers. Colorectal tumorigenesis is promoted by chronic inflammation of the intestine, and patients suffering from Crohn's disease or ulcerative colitis have an increased risk of developing colorectal cancer. Genetically engineered mice are invaluable tools for deciphering the mechanisms underpinning cancer development and provide a means to test new anti-cancer drugs.

Results

To mimic sporadic colon cancer in humans, a truncated ΔN(1-131)β-catenin was introduced as a knockin transgene into the intestinal gene-specific *gpA33* locus and combined with various oncogenic driver mutations. The resulting *gpA33*$^{\Delta N\text{-}Bcat}$ mice show increased constitutive Wnt/β-catenin pathway activation in the intestinal epithelium and spontaneously develop aberrant crypt foci and adenomatous polyps, at frequencies and latencies akin to that observed in sporadic colon cancer in humans. Consistent with this, the Wnt target genes, MMP7 and Tenascin-C, which are expressed highest in benign human adenomas and early tumor stages, were up-regulated in pre-malignant tissue of *gpA33*$^{\Delta N\text{-}Bcat}$ mice. Moreover, intestinal permeability in *gpA33*$^{\Delta N\text{-}Bcat}$ mice was increased resulting in mild chronic intestinal inflammation and increased susceptibility to azoxymethane and mutant *Apc*-dependent tumorigenesis.

Implications and future directions

The *gpA33*$^{\Delta N\text{-}Bcat}$ mice provide a model, which better mimics some aspects of sporadic colon cancer induction in humans in terms of tumor multiplicity and latency, and site-specific (i.e. colon) tumor occurrence that coincides with upregulation of markers for human colorectal cancer progression. Therefore the *gpA33*$^{\Delta N\text{-}Bcat}$ mice are likely to be useful to functionally

assess and identify mutations that co-operate with canonical Wnt/ β-catenin signaling during the initiation of adenoma formation. In turn, this is likely to identify components that constitute novel pharmacological targets for the treatment and prevention of sporadic colon cancer in humans.